

## Electronic Supplementary Information (ESI)

### Field-induced slow relaxation of magnetisation in two one-dimensional homometallic dysprosium(III) complexes based on alpha- and beta-amino acids

Marta Orts-Arroyo, Isabel Castro,<sup>\*</sup> Francesc Lloret and José Martínez-Lillo<sup>\*</sup>

*Instituto de Ciencia Molecular (ICMol), c/ Catedrático José Beltrán 2, 46980, Paterna, València, Spain.  
E-mail: f.jose.martinez@uv.es.*

Table of contents	page
Figure S1.....	2
Figure S2.....	3
Table S1.....	4
Table S2.....	5
Table S3.....	6
Figure S3.....	7
Figure S4.....	7
Table S4.....	8
Table S5.....	8
Figure S5.....	9
Figure S6.....	10
Figure S7.....	11
Figure S8.....	12

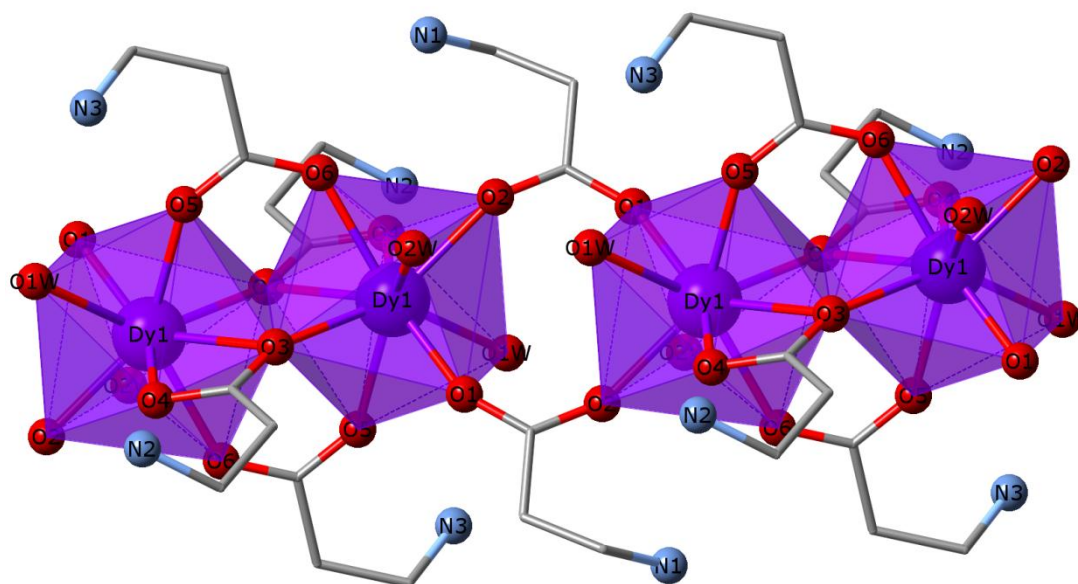
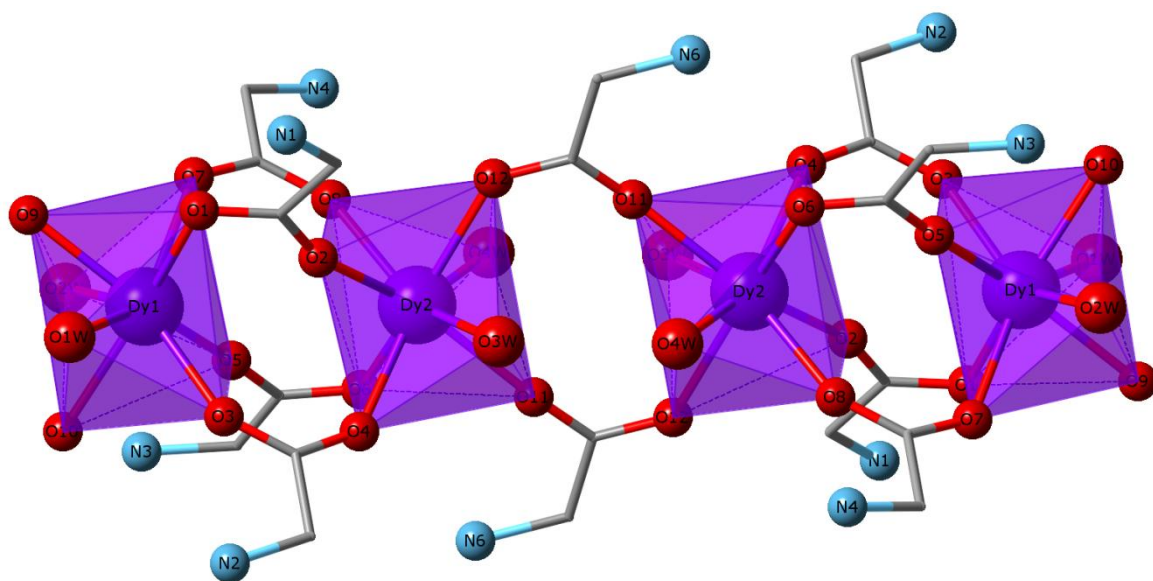


**Figure S1.** View of neighbouring dinuclear [Dy<sup>III</sup>]<sub>2</sub><sup>6+</sup> units connected through additional carboxylate groups from glycine (1, top) and β-alanine (2, bottom) amino acids that generate a cationic 1D system.

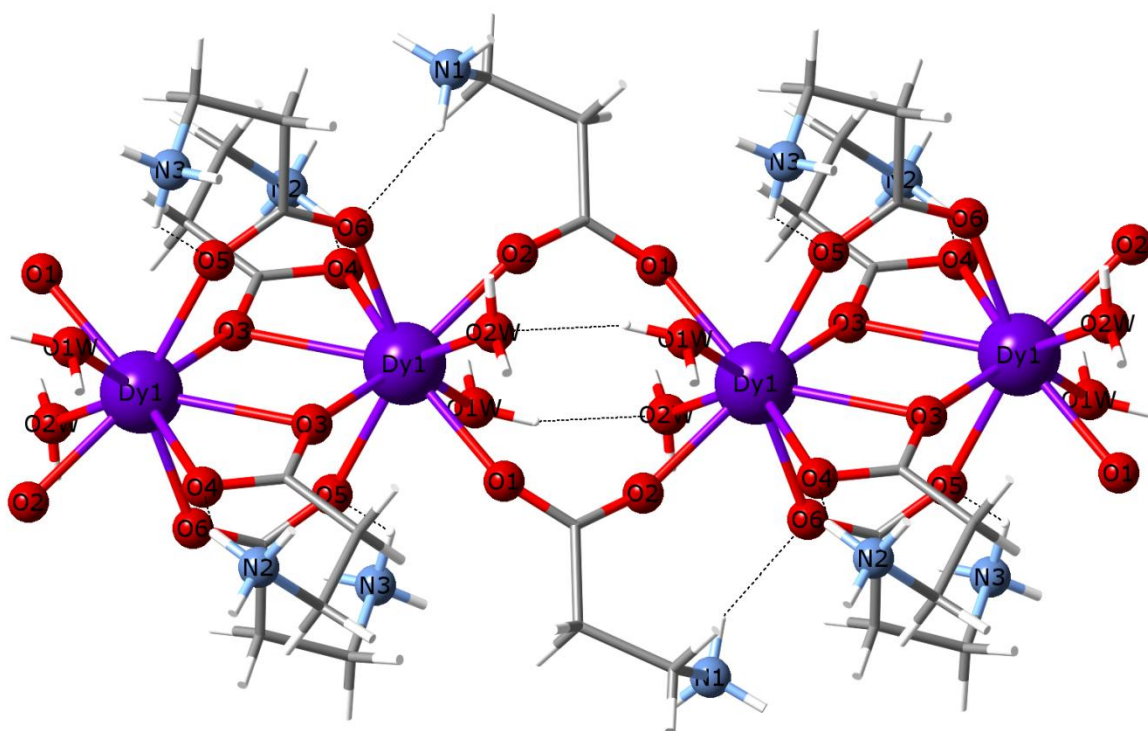


**Figure S2.** Detail of intramolecular H-bonding interactions between coordinated water molecules and also between O atoms of carboxylate and protonated  $\text{-NH}_2$  groups, which connect further the neighbouring dinuclear  $[\text{Dy}^{\text{III}}_2]^{6+}$  units in **2**.

**Table S1. Selected bond lengths (Å) for compounds 1 and 2.**

Compound	1	2
Dy(1)-O(1)	2.470(2)	2.286(2)
Dy(1)-O(2)	2.882(2)	2.327(2)
Dy(1)-O(3)	2.337(2)	2.317(2)
Dy(1)-O(4)		2.455(2)
Dy(1)-O(5)	2.291(2)	2.363(2)
Dy(1)-O(6)		2.387(2)
Dy(1)-O(7)	2.369(2)	
Dy(1)-O(9)	2.285(2)	
Dy(1)-O(1w)	2.495(2)	2.516(2)
Dy(1)-O(2w)	2.537(2)	2.524(2)
Dy(2)-O(3w)	2.501(2)	2.487(2)
Dy(2)-O(4w)	2.395(2)	2.493(2)
Dy(2)-O(2)	2.281(2)	
Dy(2)-O(4)	2.336(2)	
Dy(2)-O(6)	2.398(2)	
Dy(2)-O(7)		2.312(2)
Dy(2)-O(8)	2.358(2)	2.322(2)
Dy(2)-O(9)		2.361(2)
Dy(2)-O(11)	2.319(2)	2.294(2)
C(1)-C(2)	1.506(3)	1.515(3)
C(5)-C(6)	1.509(3)	1.515(3)
C(11)-C(12)	1.517(3)	1.516(4)
C(3)-N(1)		1.495(3)
C(4)-N(2)	1.489(3)	
C(6)-N(2)		1.499(3)
C(6)-N(3)	1.485(3)	
C(1)-O(1)	1.255(3)	1.257(3)
C(1)-O(2)	1.257(3)	1.259(3)

**Table S2. Hydrogen-Bonding Interactions in 1<sup>a</sup>.**

D-H...A	D-H/Å	H...A/Å	D...A/Å	(DHA)/°
N(1)-H(1A)...O(13c)	0.910	2.08(1)	2.944(1)	158.1(1)
N(1)-H(1A)...O(31d)	0.910	2.45(1)	2.980(1)	117.5(1)
N(1)-H(1B)...O(30e)	0.910	2.32(1)	2.954(1)	126.6(1)
N(1)-H(1C)...O(16c)	0.910	2.56(1)	3.022(1)	112.2(1)
N(1)-H(1C)...O(20)	0.910	2.28(1)	3.014(1)	137.3(1)
N(2)-H(2A)...O(21)	0.910	2.09(1)	2.933(1)	152.7(1)
N(2)-H(2A)...O(33a)	0.910	2.56(1)	3.014(1)	111.5(1)
N(2)-H(2B)...O(9w)	0.910	1.94(1)	2.841(1)	172.7(1)
N(3)-H(3A)...O(22f)	0.910	2.10(1)	2.936(1)	152.4(1)
N(3)-H(3C)...O(24)	0.910	2.14(1)	2.929(1)	144.9(1)
N(4)-H(4A)...O(5w)	0.910	2.03(1)	2.866(1)	152.9(1)
N(4)-H(4B)...O(6wb)	0.910	1.95(1)	2.847(1)	166.6(1)
N(4)-H(4C)...O(30)	0.910	2.05(1)	2.891(1)	154.2(1)
N(5)-H(5A)...O(31d)	0.910	2.53(1)	2.995(1)	112.3(1)
N(5)-H(5B)...O(27g)	0.910	2.13(1)	2.986(1)	157.1(1)
N(6)-H(6A)...O(25)	0.910	2.30(1)	2.843(1)	118.4(1)
N(6)-H(6B)...O(6)	0.910	2.01(1)	2.914(1)	174.6(1)
N(6)-H(6C)...O(8w)	0.910	1.87(1)	2.771(1)	168.8(1)
O(1w)-H(1wA)...O(9w)	0.900	1.87(1)	2.734(1)	159.4(1)
O(2w)-H(2wA)...O(1wa)	0.898	1.95(1)	2.842(1)	175.1(1)
O(2w)-H(2wB)...O(17h)	0.891	2.28(1)	2.912(1)	127.4(1)
O(3w)-H(3wA)...O(7w)	0.900	1.89(1)	2.765(1)	165.2(1)
O(3w)-H(3wB)...O(19)	0.898	1.98(1)	2.855(1)	166.3(1)
O(4w)-H(4wA)...O(5w)	0.899	1.89(1)	2.783(1)	173.2(1)
O(4w)-H(4wB)...O(3wb)	0.902	1.89(1)	2.774(1)	167.3(1)
O(5w)-H(5wB)...O(28)	0.923	2.01(1)	2.914(1)	165.5(1)
O(7w)-H(7wA)...O(28e)	0.901	2.03(1)	2.881(1)	157.2(1)
O(7w)-H(7wB)...O(6w)	0.885	2.00(1)	2.876(1)	170.3(1)
O(8w)-H(8wA)...O(7w)	0.930	1.87(1)	2.779(1)	166.5(1)
O(9w)-H(9wA)...O(16)	0.860	1.99(1)	2.841(1)	168.5(1)
O(9w)-H(9wB)...O(20)	0.923	1.94(1)	2.843(1)	164.5(1)

<sup>a</sup>Symmetry codes: (a) = -x+1, -y, -z+1; (b) = -x+2, -y+1, -z+1; (c) = -x+2, -y, -z+1; (d) = -x+1, -y, -z+2; (e) = x+1, y, z; (f) = -x+1, -y+1, -z+1; (g) = x, y-1, z; (h) = x-1, y, z.

**Table S3. Hydrogen-Bonding Interactions in 2<sup>a</sup>.**

D-H...A	D-H/Å	H...A/Å	D...A/Å	(DHA)/°
N(1)-H(01A)...O(20)	0.910	2.03(1)	2.854(1)	150.5(1)
N(1)-H(01B)...O(2)	0.910	2.25(1)	2.858(1)	123.5(1)
N(1)-H(01B)...O(6f)	0.910	2.11(1)	2.943(1)	151.3(1)
N(1)-H(01C)...O(14g)	0.910	2.42(1)	2.959(1)	118.0(1)
N(2)-H(02A)...O(32h)	0.910	2.05(1)	2.944(1)	168.7(1)
N(2)-H(02B)...O(4)	0.910	2.15(1)	2.818(1)	129.3(1)
N(2)-H(02C)...O(35)	0.910	2.33(1)	2.902(1)	120.7(1)
N(3)-H(03A)...O(5)	0.910	2.17(1)	2.762(1)	122.0(1)
N(3)-H(03C)...O(14g)	0.910	2.44(1)	3.023(1)	122.6(1)
N(3)-H(03C)...O(15g)	0.910	2.05(1)	2.954(1)	170.8(1)
N(4)-H(04B)...O(10f)	0.910	2.03(1)	2.885(1)	156.1(1)
N(5)-H(05A)...O(9)	0.910	2.05(1)	2.738(1)	131.0(1)
N(5)-H(05B)...O(5we)	0.910	1.95(1)	2.858(1)	172.1(1)
N(5)-H(05C)...O(28d)	0.910	2.18(1)	2.948(1)	142.0(1)
N(6)-H(06A)...O(34i)	0.910	2.26(1)	2.941(1)	131.7(1)
N(6)-H(06B)...O(26e)	0.910	2.23(1)	2.997(1)	142.1(1)
N(6)-H(06C)...O(12)	0.910	2.17(1)	2.829(1)	128.8(1)
N(6)-H(06C)...O(33e)	0.910	2.15(1)	2.952(1)	147.2(1)
O(1w)-H(1wA)...O(25c)	0.893	2.14(1)	2.989(1)	159.8(1)
O(1w)-H(1wB)...O(25c)	0.890	2.06(1)	2.887(1)	154.0(1)
O(2w)-H(2wA)...O(28)	0.926	1.96(1)	2.861(1)	164.3(1)
O(2w)-H(2wB)...O(14e)	0.902	2.58(1)	2.584(1)	127.4(1)
O(2w)-H(2wB)...O(16e)	0.902	2.15(1)	3.022(1)	162.8(1)
O(3w)-H(3wA)...O(35)	0.889	2.06(1)	2.927(1)	163.9(1)
O(3w)-H(3wB)...O(23e)	0.921	1.87(1)	2.778(1)	167.7(1)
O(4w)-H(4wA)...O(3wd)	0.883	2.19(1)	2.943(1)	142.5(1)
O(4w)-H(4wA)...O(8)	0.883	2.29(1)	3.030(1)	141.5(1)
O(4w)-H(4wB)...O(33d)	0.888	2.03(1)	2.889(1)	162.8(1)

<sup>a</sup>Symmetry codes: (c) = -x+1, -y+1, -z+2; (d) = -x+2, -y+2, -z+1; (e) = x+1, y, z; (f) = x-1, y, z; (g) = -x, -y+1, -z+2; (h) = -x+2, -y+1, -z+1; (i) = -x+3, -y+1, -z+1.

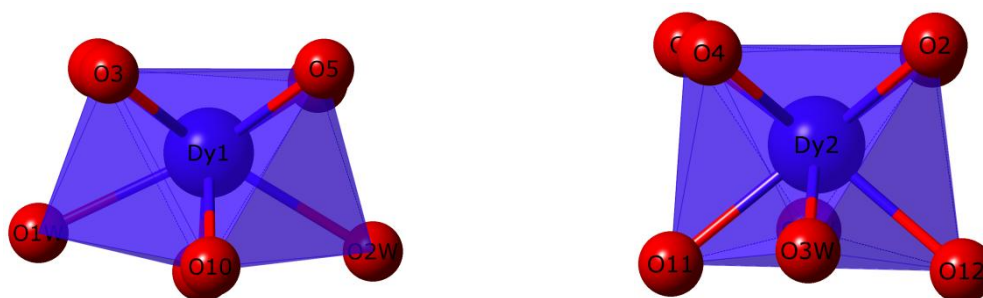


**Figure S3.** Perspective view of the environment of the dysprosium atoms of the dinuclear  $[\text{Dy}^{\text{III}}_2]^{6+}$  unit in compound **1** [Dy(1), left; Dy(2), right].

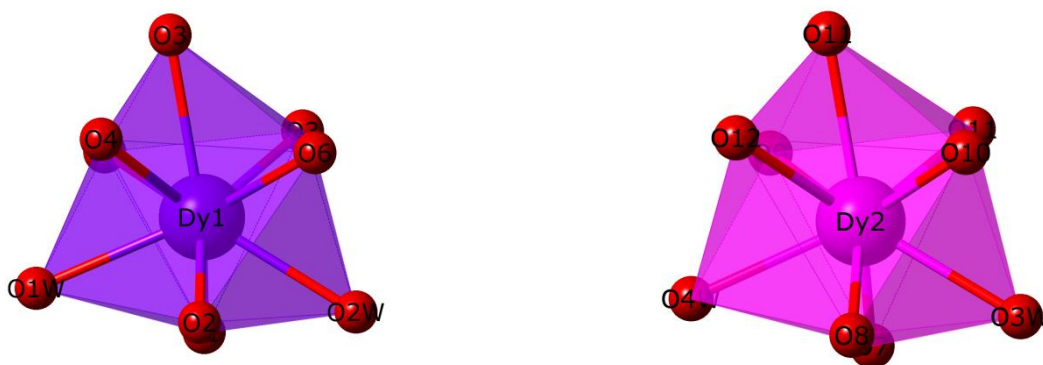


**Figure S4.** Perspective view of the environment of the dysprosium atoms of the dinuclear  $[\text{Dy}^{\text{III}}_2]^{6+}$  units in compound **2** [Dy(1), left; Dy(2), right].

**Table S4. Selected Structural Data for 1<sup>a</sup>**

	Dy(1)	Dy(2)
S(SAPR) <sup>b</sup>	1.207	0.882
S(BCTPR) <sup>c</sup>	0.712	1.170
M–O <sup>d</sup> (Å)	2.470	2.398
M–O <sup>e</sup> (Å)	2.324	2.334
M–O <sub>w</sub> <sup>f</sup> (Å)	2.516	2.448
O–M–O <sup>g</sup> (°)	123.67	122.35
Δ <sup>h</sup> (Å)	0.01	0.01
δ <sup>g</sup> (°)	170.26	164.95
δ <sup>h</sup> (°)	18.27	20.66
τ <sup>i</sup> (°)	2.54	5.70
τ <sup>j</sup> (°)	42.95	49.50
v/h <sup>k</sup>	1.089	1.059
v/h <sup>l</sup>	0.997	1.039

<sup>a</sup> Selected structural data for the two crystallographically independent dysprosium atoms (Dy1 and Dy2) for compound 1. <sup>b</sup> Value of the SHAPE parameter relative to the ideal spherical version of the square antiprismatic (SAPR) polyhedron. <sup>c</sup> Value of the SHAPE parameter relative to the ideal spherical version of the bicapped trigonal prismatic (BCTPR) polyhedron. <sup>d</sup> Value of the long metal-oxygen bond length from the carboxylate group. <sup>e</sup> Average value of the short metal-oxygen bond lengths from the carboxylate groups. <sup>f</sup> Average value of the metal-oxygen bond lengths from the coordinated water molecules. <sup>g</sup> Value of the metal-oxygen bond angles from the capping oxygen atoms. <sup>h</sup> Value of the metal deviation from the mean plane formed by the capping oxygen atoms. <sup>i</sup> Value of the dihedral angle between the two opposite triangular faces of the BCTPR. <sup>j</sup> Value of the dihedral angle between the two adjacent triangular prismatic faces of the basal square face of the SAPR. <sup>k</sup> Value of the trigonal twist angle between the two opposite basal triangular faces of the BCTPR. <sup>l</sup> Value of the tetragonal twist angle between the two opposite basal square faces of the SAPR. <sup>k</sup> Values of the compression (or elongation) parameter of the lateral rectangular faces of the BCTPR. <sup>l</sup> Values of the compression (or elongation) parameter of the lateral triangular faces of the SAPR.

**Table S5. Selected Structural Data for 2<sup>a</sup>**

	Dy(1)	Dy(2)
S(CSAPR) <sup>b</sup>	1.091	1.186
S(TCTPR) <sup>c</sup>	1.530	1.541
M–O <sup>d</sup> (Å)	2.597	2.550
M–O <sup>e</sup> (Å)	2.356	2.360
M–O <sub>w</sub> <sup>f</sup> (Å)	2.520	2.490
O–M–O <sup>g</sup> (°)	103.0/125.2/130.8	104.9/124.8/126.6
Δ <sup>h</sup> (Å)	0.140	0.112
δ <sup>g</sup> (°)	169.12	170.82
δ <sup>h</sup> (°)	19.06	22.28
τ <sup>i</sup> (°)	6.20	5.02
τ <sup>j</sup> (°)	44.44	42.975
v/h <sup>k</sup>	1.12	1.08
v/h <sup>l</sup>	0.98	0.99

<sup>a</sup> Selected structural data for the two crystallographically independent dysprosium atoms (Dy1 and Dy2) for compound 2. <sup>b</sup> Value of the SHAPE parameter relative to the ideal spherical version of the capped square antiprismatic (CSAPR) polyhedron. <sup>c</sup> Value of the SHAPE parameter relative to the ideal spherical version of the tricapped trigonal prismatic (TCTPR) polyhedron. <sup>d</sup> Value of the long metal-oxygen bond length from the carboxylate group. <sup>e</sup> Average value of the short metal-oxygen bond lengths from the carboxylate groups. <sup>f</sup> Average value of the metal-oxygen bond lengths from the coordinated water molecules. <sup>g</sup> Values of the metal-oxygen bond angles from the three capping oxygen atoms of the TCTPR. <sup>h</sup> Value of the metal deviation from the mean plane formed by the three capping oxygen atoms of the TCTPR. <sup>i</sup> Value of the dihedral angle between the two opposite triangular faces of the TCTPR. <sup>j</sup> Value of the dihedral angle between the two adjacent triangular prismatic faces of the basal square face of the CSAPR. <sup>k</sup> Value of the trigonal twist angle between the two opposite basal triangular faces of the TCTPR. <sup>l</sup> Value of the tetragonal twist angle between the two opposite basal square faces of the CSAPR. <sup>k</sup> Values of the compression (or elongation) parameter of the lateral rectangular faces of the TCTPR. <sup>l</sup> Values of the compression (or elongation) parameter of the lateral triangular faces of the CSAPR.



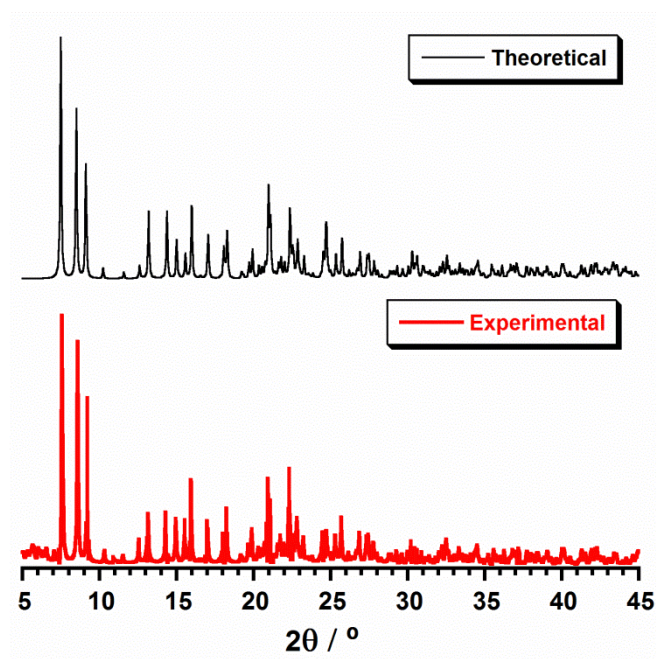
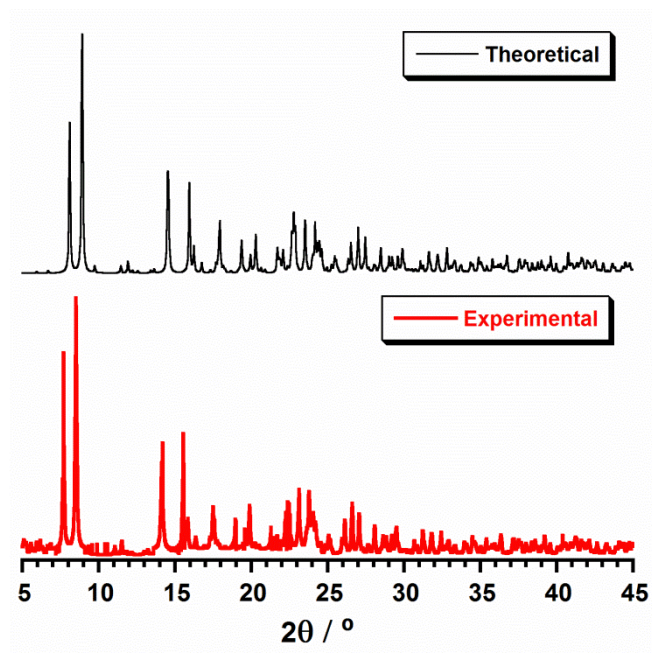


**Figure S5.** Plots of the theoretical and experimental XRD patterns profile ( $2\theta/^\circ$ ) in the range 5-45° for compounds **1** (top) and **2** (bottom).

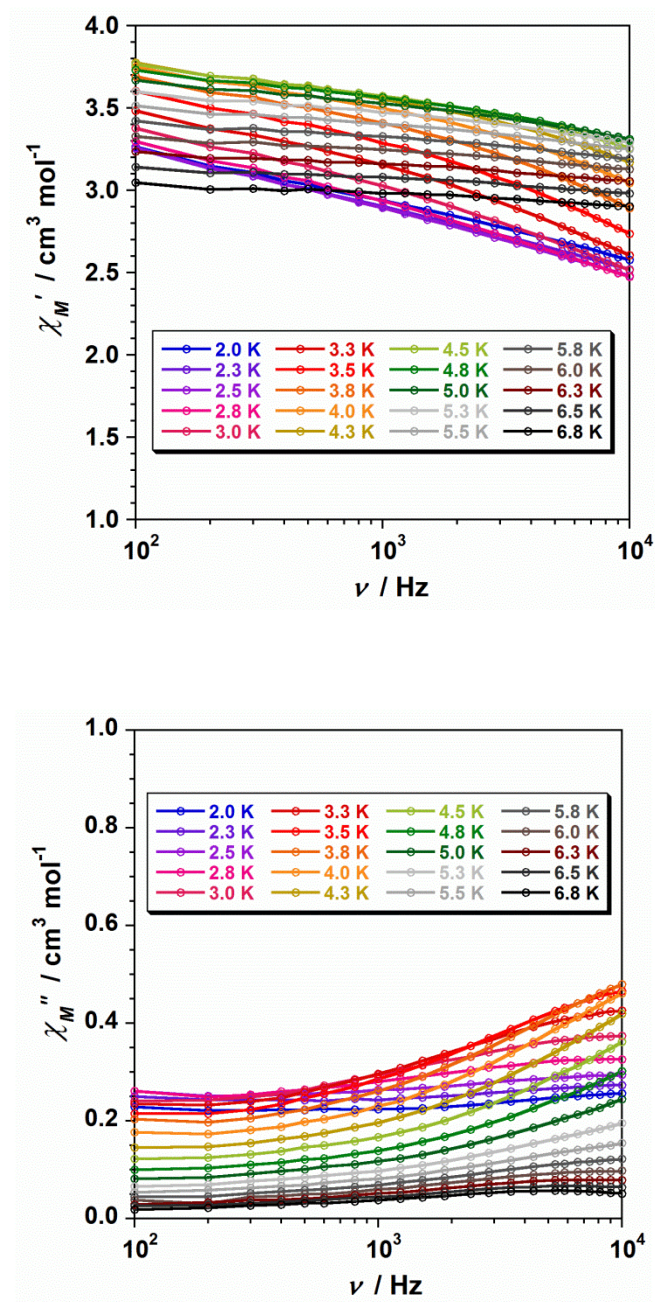


**Figure S6.** Frequency dependence of the in-phase (top) and out-of-phase (bottom) *ac* magnetic susceptibility signals for compound **1** under a dc field of 2500 G.

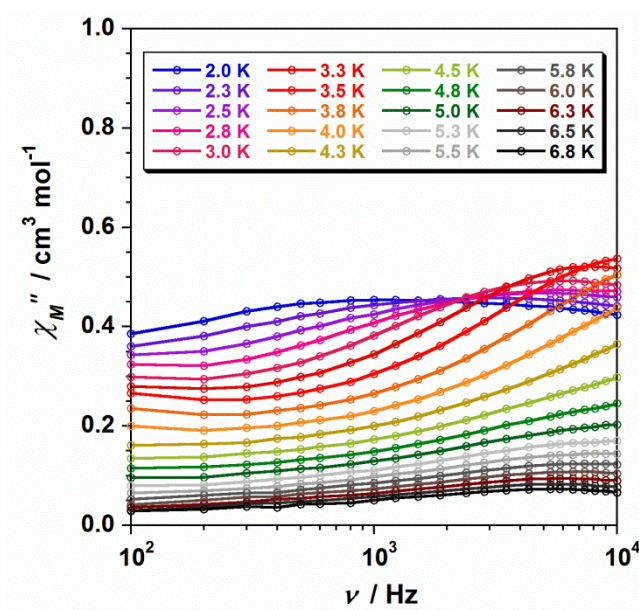
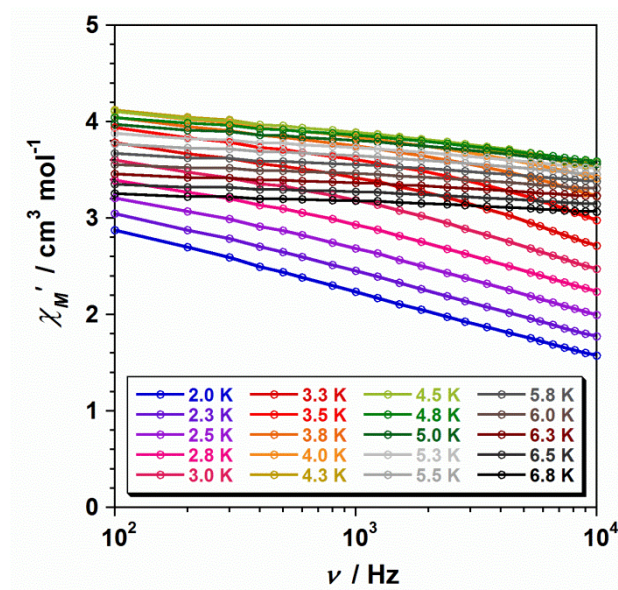


**Figure S7.** Frequency dependence of the in-phase (top) and out-of-phase (bottom) *ac* magnetic susceptibility signals for compound **2** under a dc field of 2500 G.

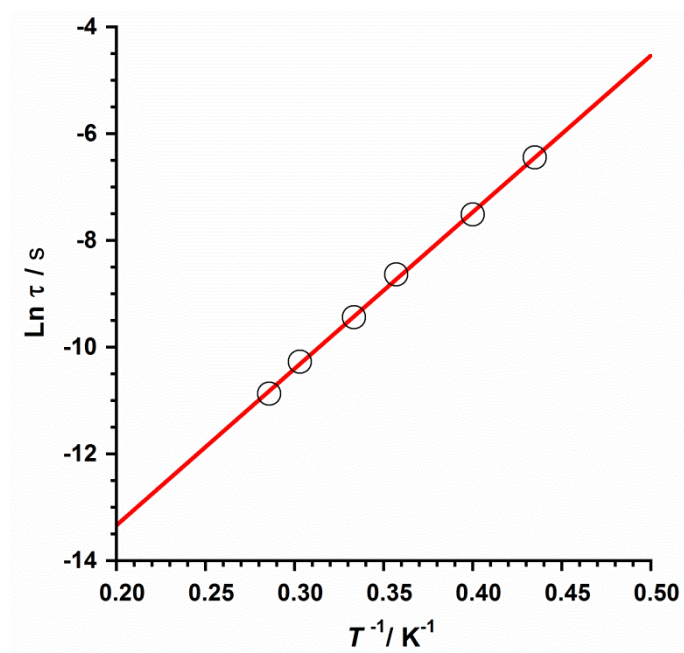


**Figure S8.**  $\ln(\tau)$  versus  $1/T$  plot for **2**, obtained with out-of-phase ac data at  $H_{dc} = 1000$  G, showing the fit to the Arrhenius law (solid line).